Technical Notes

TECHNICAL NOTES are short manuscripts describing new developments or important results of a preliminary nature. These Notes cannot exceed 6 manuscript pages and 3 figures; a page of text may be substituted for a figure and vice versa. After informal review by the editors, they may be published within a few months of the date of receipt. Style requirements are the same as for regular contributions (see inside back cover).

A Comparison of Scramjet Integral Analysis Techniques

G. A. Sullins* and P. J. Waltrup†
The Johns Hopkins University
Applied Physics Laboratory, Laurel, Maryland

Introduction

THE aerothermodynamic analysis of supersonic combustion ramjet (scramjet) engines using integral techniques has evolved along three paths since the inception of this propulsion concept in the late 1950's. All three approaches use the governing conservation equations of mass, momentum, and energy plus an equation of state but vary in their treatment of the closure required to obtain a solution for the supersonic combustor, including the treatment of combustion induced compression fields.

In the first approach (see, e.g., Refs. 1 and 2), an a priori knowledge of a physical property such as static pressure, total temperature, heat release, etc., within the combustor is required to obtain a solution. Generally, these properties are obtained from experiments and do not discriminate between the compression field generated within the supersonic combustor and that generated by the combustion process at or near the entrance of the combustor. However, these approaches are able to accurately predict the measured combustor exit flow properties from these same experiments plus other, closely related, experiments.

The other two approaches to closure do not require an a priori knowledge of properties within the supersonic combustor and are, therefore, preferable to one that does. The first of these is the simpler of the two in that a prime variable, such as pressure, Mach number, area, or density, is held constant (see, e.g., Refs. 3-6). However, these approaches are limited in their ability to treat the precombustion compression process, i.e., they treat only the no-shock and normal shock cases, and do not, in general, compare favorably with experimental data.

The third approach[7-9] is one in which a Crocco power law relationship between static pressure and area is assumed, i.e., $PA^{\epsilon/(\epsilon-1)} = \text{const}$. The constant area and constant Mach number processes can be shown to be special cases of this method. Moreover, no a priori knowledge of combustor properties is necessary. This approach permits inclusion and prediction of the strength of the precombustion compression field as a function of heat release and compares favorably with a diverse cross section of experimental data.[9-11] Thus, this is the preferred approach for prediction of scramjet performance.

Although the power law representation is the preferred approach, some investigations still use the constant property approach to predict scramjet performance for simplicity. The purpose of this Note is to illustrate the differences in predicted engine performance that can arise if the constant area or constant Mach number assumptions are used rather than the more realistic power law representation.

Engine/Cycle Analysis

Figure 1 is a schematic representation of the scramjet used in this study, and is a generic derivative of some recent scramjet-powered vehicle concepts. It has an inlet area A_i of 645 cm^2 (100 in.^{2}), an inlet contraction ratio A_i/A_{ci} of 5.824, a combustor exit-to-inlet area ratio A_{ce}/A_{ci} of 3.0, and a nozzle exit-to-inlet area ratio A_{ex}/A_i of 1.7. The 94-cm (37-in.)-long combustor consists of a 19-cm (7.5-in.)-long con-

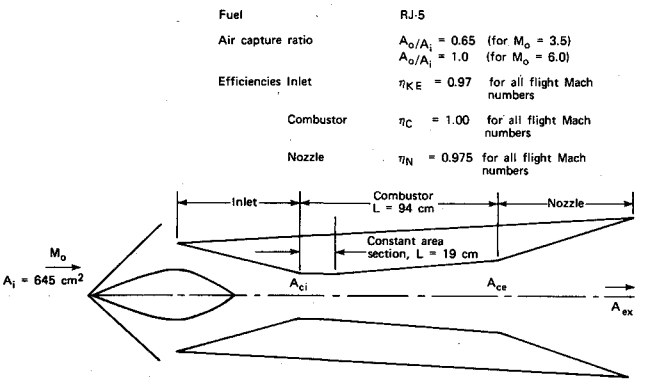

Fig. 1 Scramjet engine configuration.

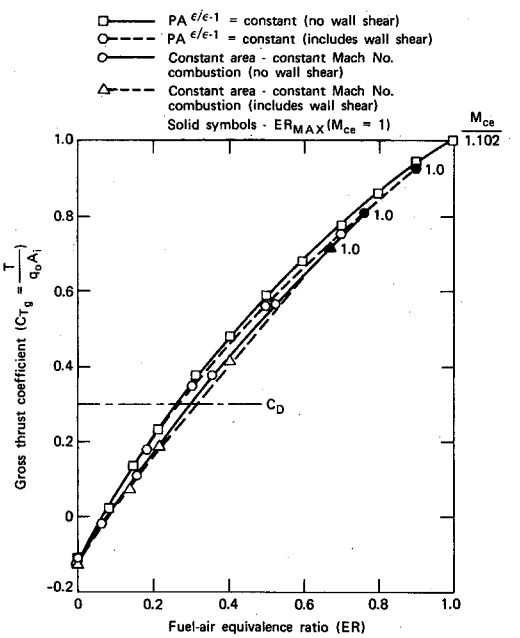

Fig. 2 Thrust coefficient vs equivalence ratio for $M=3.5$ flight at 10,000 ft altitude.

Received April 12, 1984; revision received Oct. 1, 1984.

*Associate Engineer, Propulsion Group. Associate Member AIAA.
†Assistant Group Supervisor for Advanced Propulsion. Associate Fellow AIAA.

stant area section followed by a truncated cone. Combustor length is specified so that the effects of wall shear losses, which can be quite large in supersonic combustors,[12] can be included in the study.

Two flight conditions were selected for this study: Mach 3.5 at 3 km (10,000 ft), representative of end-of-boost; and Mach 6 at 15.2 km (50,000 ft) representative of cruise; which are typical conditions for current liquid/fueled scramjet-powered concepts. At Mach 3.5, the inlet air capture ratio A_0/A_i is taken to be 0.65; at Mach 6.0, the ratio is 1.0. The inlet kinetic energy efficiency, fuel combustion efficiency, and exit nozzle efficiency are taken to be 0.97, 1.0, and 0.975, respectively, at both flight conditions. The fuel used in all cases is Shelldyne-H (RJ-5).

The cycle analysis used (described in detail in Ref. 9) utilizes the conservation equations (mass, momentum, and energy) and an equation of state. Two approaches are compared for computing the combustion process in a scramjet engine. The first method consists of two processes: a constant area combustion process in which sufficient fuel is added to decelerate the supersonic flow entering the combustor to a desired Mach number, and a constant Mach number combustion process in which fuel is added such that the Mach number in the diverging combustor section remains constant. For this method, the constant property assumptions provide closure of the equations, i.e., constant area eliminates the $\int P dA$ term in the momentum equation and constant Mach number provides a known exit property. This method, however, does not allow for any shock system prior to combustion other than a normal shock. If a normal shock precedes combustion, the flow will be subsonic throughout the combustor unless it is increased to $M=1.0$ at the exit of the constant area section. However, this results in the same case as that of no shock and decreasing the Mach number to $M=1.0$ through heat addition in the constant area section.

The second method is based upon the Crocco pressure-area relationship $PA^{\epsilon/\epsilon-1}=\text{const}$, with ϵ being determined by the entropy limit constraint, i.e., the entropy rise is minimized through the combustor with the slope of the isentrope matching that of the combustor exit conditions. This allows the determination of the integral term $\int P dA$, thus providing closure of the equations. This process allows for a shock system (either normal, oblique, or no shock wave) at the combustor entrance. For both methods, equilibrium chemistry is assumed throughout the engine except in the exit nozzle, where two-thirds of the flow is assumed frozen.

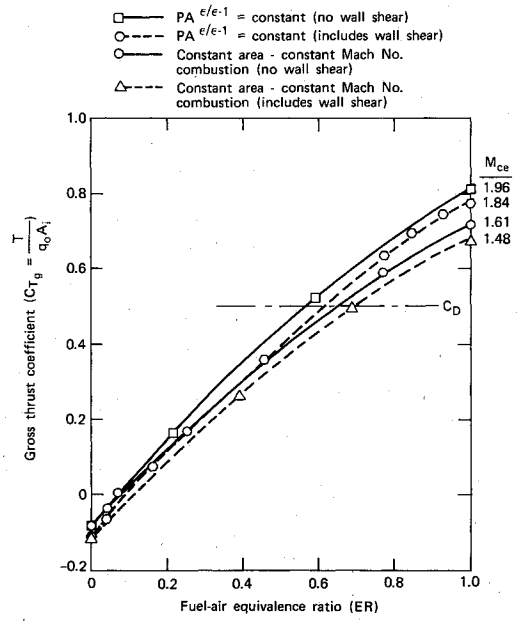

Fig. 3 Thrust coefficient vs equivalence ratio for $M=6.0$ flight at 50,000 ft altitude.

For the Mach 3.5 case, the highest thrust coefficient and fuel-air equivalence ratios, ER, are obtained assuming sufficient heat is added in the constant area section to choke the flow, permitting the presence of either no shock or a normal shock. If less heat is added in the constant area section, a normal shock cannot be present (since $M \geq 1$) and the maximum ER and thrust coefficient is decreased. More heat cannot be added. However, at Mach 6, the maximum thrust coefficients are obtained when no shock is present and when sufficient heat is added in the constant area and conical sections to permit $ER=1$ to be reached at the exit of the combustor. If more heat is added in the constant area section, then $ER=1$ is reached prior to exiting the conical section and the process in the conical combustor section is no longer constant Mach number. If less heat is added, then $ER<1$ at the exit of the combustor.

Results

Figures 2 and 3 present the computed gross thrust coefficients (C_{Tg}) as a function of ER for the Mach 3.5 and 6 cases, respectively. The solid lines exclude the effects of combustor wall shear and the dashed lines include them. Combustor exit Mach numbers M_{ce} are listed to the right of each curve. Typical cruise drag coefficients C_D at each condition are also included for reference (dash-dot lines).

At Mach 3.5 and 3 km (10,000 ft) altitude, Fig. 2 shows that without the inclusion of wall shear (solid lines), the constant property assumption overpredicts the amount of fuel required to overcome drag by 15% ($ER=0.3$ vs 0.26) and underpredicts the maximum thrust coefficient by 23%. The latter is due mainly to the maximum amount of heat that can be added prior to thermal choking at the combustor exit ($ER_{\max}=0.76$ for the constant area/Mach number assumption vs 1.0 using the Crocco relationship). With combustor wall shear included (dashed lines), these differences are even more pronounced, the percentages being 18% and 30%, respectively.

At Mach 6 (Fig. 3), a similar trend is present, although the maximum ER in all cases is unity. Without combustor wall shear, the constant area/Mach number closure assumption overpredicts the fuel flow required for cruise by 14% and underpredicts the maximum C_{Tg} by 14%. With wall shear included, the percentages are 11% and 15%, respectively.

The effect of combustor wall shear for a given closure rule is also worthy of discussion because it has such a significant effect on engine performance. When the experimentally verified Crocco closure is used, the effect of wall shear at Mach 3.5 is to increase the predicted ER required to overcome drag by 4% but reduce the maximum C_{Tg} by 8% because thermal choking is encountered. At Mach 6, the inclusion of combustor wall shear increases the ER at cruise by 9% and reduces $C_{Tg_{\max}}$ by 6%.

Concluding Remarks

Two integral analysis methods are compared for estimating the performance characteristics of a scramjet engine. The first method is a two-step process, assuming constant area combustion followed by constant Mach number combustion. The second is a one-step process in which combustion is assumed to follow a Crocco pressure-area relationship, $PA^{\epsilon/\epsilon-1}=\text{const}$, and has been experimentally verified under a variety of test conditions. Thrust coefficients are compared for both methods at flight conditions of $M_0=3.5$, $z=3$ km (10,000 ft) and $M_0=6$, $z=15.2$ km (50,000 ft). The results show that the constant property process underpredicts the expected engine performance, especially at the low flight Mach number. Although the absolute values will change from configuration to configuration, the relative differences will remain the same.

References

[1] Cookson, R. A., "An Analysis of Non-Constant Area Heat Addition Due to Combustion in a Supersonic Air-Steam," U.S. Air Force Office of Scientific Research Interim Scientific Report AFOSR-TR-75-1483, Sept. 1975.

[2] Pinckney, S. Z., "Integral Performance Predictions for Langley Scramjet Engine Module," NASA TM-X-74038, Jan. 1978.

[3] Ferri, A., Libby, P., and Zakkay, V., "Theoretical and Experimental Investigation of Supersonic Combustion," *Proceedings, 3rd Congress ICAS*, 1962, MacMillan Press, London, 1964, pp. 1089-1156.

[4] Hsia, H. T. S., "A Criteria for the Combustion Modes in Constant Area Combustors," ASME Paper 70-WA/AV-4, 1970.

[5] Henry, J. R. and Anderson, G. Y., "Design Considerations for the Airframe Integrated Scramjet," *Ist International Symposium on Air Breathing Engine*, Marseille, France, June 1972; also NASA TM-X-2895, 1973.

[6] Bussing, T. R. A. and Murman, E. M., "A One-Dimensional Unsteady Model of Dual Mode Scramjet Operation," AIAA Paper 83-0422, Jan. 1983.

[7] Billig, F. S. and Dugger, G. L., "The Interaction of Shock Waves and Heat Addition in the Design of Supersonic Combustors," *Twelfth Symposium (International) on Combustion*, The Combustion Institute, Pittsburgh, Pa., 1969, p. 1125.

[8] Waltrup, P. J. and Billig, F. S., "Prediction of Precombustion Wall Pressure Distributions in Scramjet Engines," *Journal of Spacecraft and Rockets*, Vol. 10, Sept. -Oct. 1973, pp. 620-622.

[9] Waltrup, P. J., Billig, F. S., and Stockbridge, R. D., "A Procedure for Optimizing the Design of Scramjet Engines," *Journal of Spacecraft and Rockets*, Vol. 16, May-June 1979, pp. 163-172.

[10] Waltrup, P. J., Dugger, G. L., Billig, F. S., and Orth, R. C., "Direct Connect Tests of Hydrogen-Fueled Supersonic Combustors," *Sixteenth Symposium (International) on Combustion*, The Combustion Institute, 1976, p. 1619.

[11] Anderson, G. Y., Eggers, J. M., Waltrup, P. J., and Orth, R. C., "Investigation of Step Fuel Injectors for an Integrated Modular Scramjet Engine," *CPIA Publication 281*, Vol. III, pp. 175-190.

[12] Waltrup, P. J., Billig, F. S., and Evans, M. C., "Critical Considerations in the Design of Supersonic Combustion Ramjet (scramjet) Engines," *Journal of Spacecraft and Rockets*, Vol. 18, July-Aug. 1981, pp. 350-356.

Heat Transfer in the Vicinity of a Large-Scale Obstruction in a Turbulent Boundary Layer

M. F. Blair*

United Technologies Research Center
East Hartford, Connecticut

Nomenclature

C_f = skin friction coefficient
H = boundary-layer shape factor, δ^*/θ
Re_θ = Reynolds number based on momentum thickness, $U_e\theta/\nu$
St = Stanton number, $h/\rho_e U_e c_p$
U_e = freestream velocity
X = distance from test section entrance
Y^+ = dimensionless distance from wall
δ = boundary-layer thickness
δ^* = boundary-layer displacement thickness
θ = boundary-layer momentum thickness

Presented as Paper 84-1723 at the AIAA 19th Thermophysics Conference, Snowmass, Colo., June 25-28, 1984; received Sept. 5, 1984. Revision received Nov. 1, 1984.

*Senior Research Engineer.

Introduction

HEAT transfer rates can be increased markedly in the region near a local obstruction in a boundary-layer flow, a manifestation of three-dimensional leading-edge horseshoe vortex effects. Examples of locations within gas turbine engines where leading-edge flow effects are known to cause increased heat transfer include the junction of airfoil leading edges with the platforms, the junction of support struts with the augmentor liner, and the region around dilution jet sites in combustors.

Leading-edge vortices develop just upstream ($\approx$1-4 obstruction widths) of an obstruction leading edge. The slower portion of the approaching boundary layer is unable to negotiate the local adverse streamwise pressure gradient and the boundary-layer fluid rolls up into a vortex oriented (at the plane of symmetry) parallel to the approach surface and perpendicular to the mainstream flow. This leading-edge vortex brings fluid with relatively high momentum nearer to the wall, increasing the velocity gradient normal to the wall and producing higher local skin friction. For flows with both velocity and temperature boundary layers, leading-edge effects produce higher local heat transfer both by increasing the local heat transfer coefficient and by transporting fluid at the freestream temperature closer to the surface.

Previous experimental work on three-dimensional flow effects near obstruction leading edges has been oriented to the study of aerodynamic effects.[1,2] An exception is the recent work by Han et al.,[3] which investigated horseshoe vortex effects on the heat transfer distribution on a cylindrical obstruction. In constrast to Ref. 3, which focused on changes to the heat transfer distribution over the obstruction surface, the present study was designed to examine the effects of a horseshoe vortex on the heat transfer to the surface beneath the approach boundary layer. The present study was designed to provide both flowfield and surface heat transfer distribution data for a fixed geometry and set of experimental test conditions.

Description of Test Equipment

This study was conducted in a low-speed, open-circuit, low-turbulence wind tunnel with a straight test section 50-cm wide, 20-cm high and 2.3-m long. The test surface along which the approach boundary layer developed consisted of the 50-cm-wide horizontal lower wall of the test section. Rods 6 mm^2 located on the top and bottom surfaces at the test section entrance tripped and artifically thickened the boundary layer.

A forward-facing rectangular block, spanning the test section from top to bottom, was mounted along the centerline 0.9 m from the test section entrance. The block was 15.2 cm wide, 90 cm long, and had a circular arc trailing edge to reduce unsteadiness in the wake. The lower wall of the test section, along with the approach boundary layer developed, was a uniform heat flux surface. This test surface consisted of a block of rigid urethane foam covered with thin (0.025 mm) stainless steel foil. Regulated d.c. current passing through the foil provided a nearly uniform surface heat flux. Local Stanton numbers were determined by measuring the local surface temperature reached with the uniform heat flux boundary condition. This particular heat transfer model fabrication technique is designed to permit measurement of local heat transfer coefficients since conduction both along the thin foil and through the rigid foam substrate is negligible.

The temperature distribution and therefore the Stanton number distribution over the uniform heat flux plate was determined using an AGA Model 780 color display scanning